

## **Electronic structure manipulation of MoSe<sub>2</sub> nanosheets with fast reaction kinetics toward long-life sodium-ion half/full batteries**

Lei Zhang<sup>a,b</sup>, Huilong Dong<sup>a</sup>, Chengkui Lv<sup>a,d</sup>, Chencheng Sun<sup>a</sup>, Huaixin Wei<sup>d</sup>,  
Xiaowei Miao<sup>a</sup>, Jun Yang<sup>c\*</sup>, Liang Cao<sup>a,e\*</sup>, Hongbo Geng<sup>a\*</sup>

<sup>a</sup>School of Materials Engineering, Changshu Institute of Technology, Changshu, Jiangsu, 215500, China.

<sup>b</sup>College of Chemistry, Chemical Engineering and Materials Science, Soochow University, Suzhou, Jiangsu, 215123, China.

<sup>c</sup>School of Material Science & Engineering, Jiangsu University of Science and Technology, Zhenjiang, 212003, China.

<sup>d</sup>School of Chemistry and Life Sciences, Suzhou University of Science and Technology, Suzhou, 215009, China.

<sup>e</sup>Key Laboratory of Advanced Energy Materials Chemistry (Ministry of Education) College of Chemistry, Nankai University, Tianjin, 300071, China.

E-mail address: [liangcao@cslg.edu.cn](mailto:liangcao@cslg.edu.cn); [iamjyang@just.edu.cn](mailto:iamjyang@just.edu.cn); [hbgeng@gdut.edu.cn](mailto:hbgeng@gdut.edu.cn).

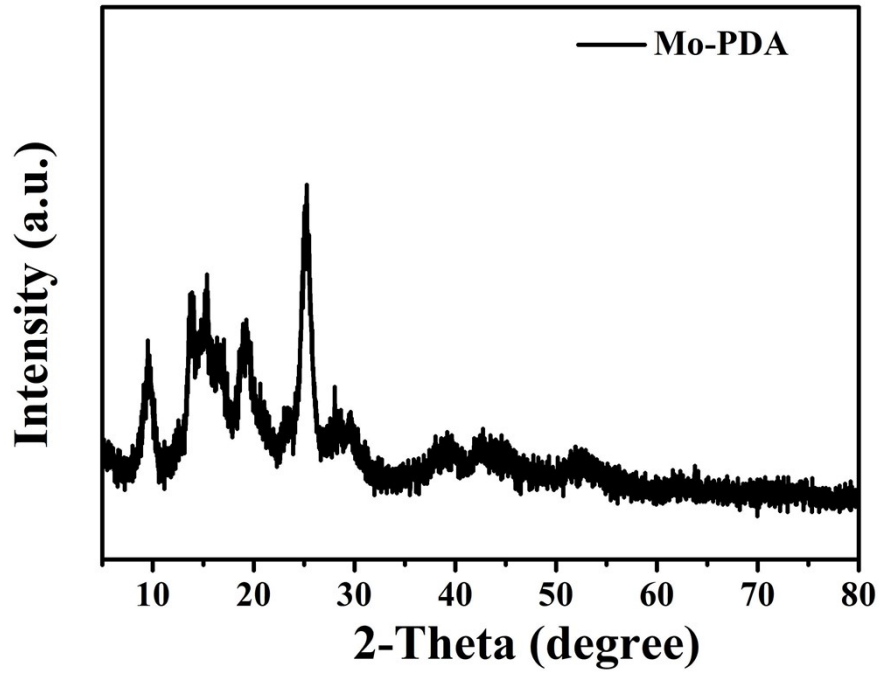


Figure S1. XRD pattern of Mo-PDA precursor.

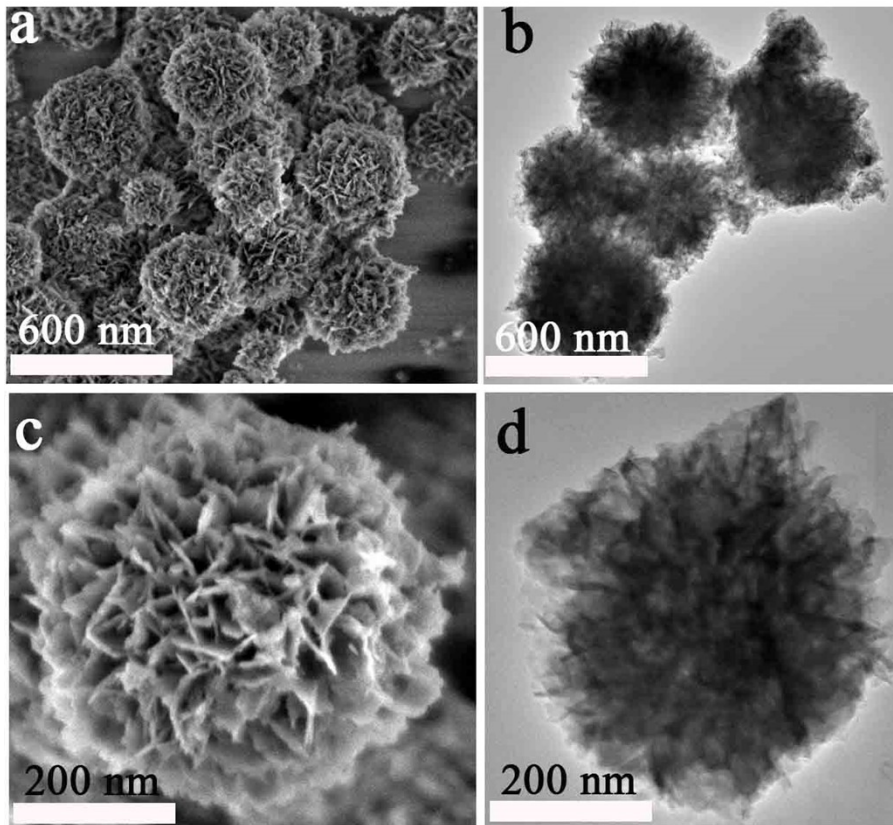
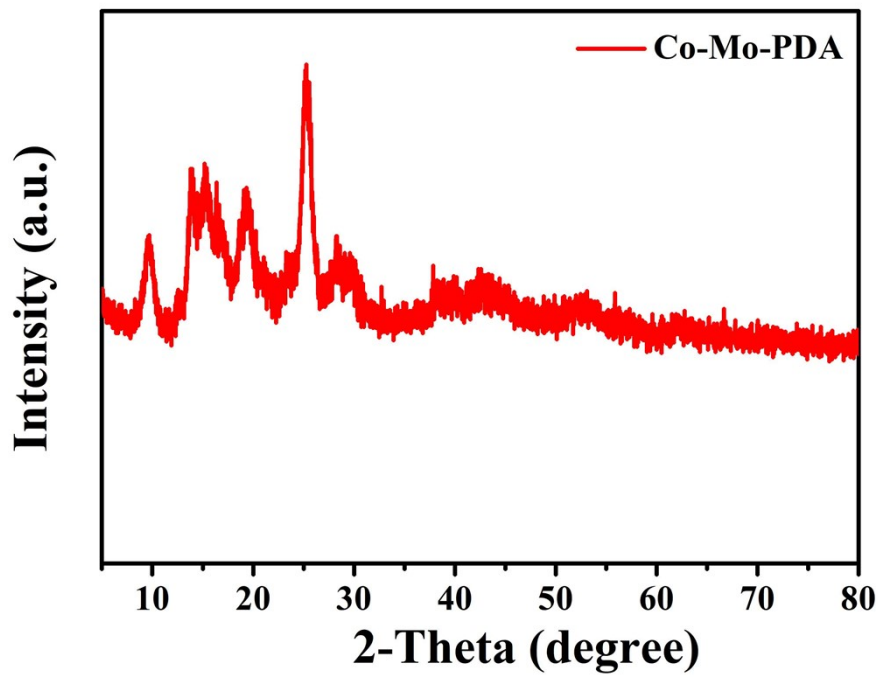
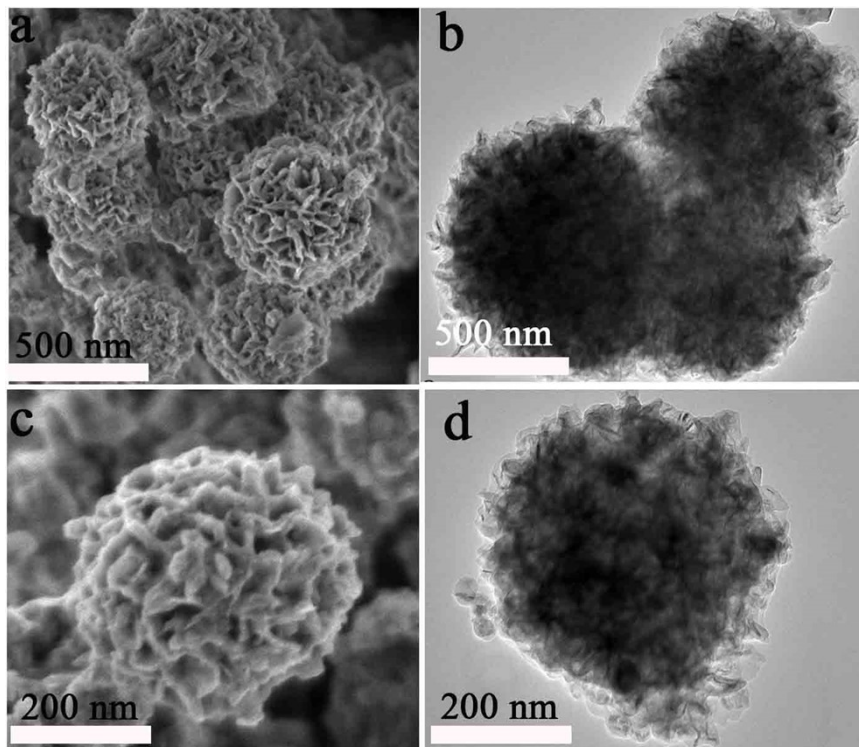


Figure S2. (a) and (c) SEM image of Mo-PDA precursor. (b) and (d) TEM image of Mo-PDA precursor.



**Figure S3.** XRD pattern of Co-Mo-PDA precursor.



**Figure S4.** (a, c) SEM image of Co-Mo-PDA precursor. (b, d) TEM image of Co-Mo-PDA precursor.

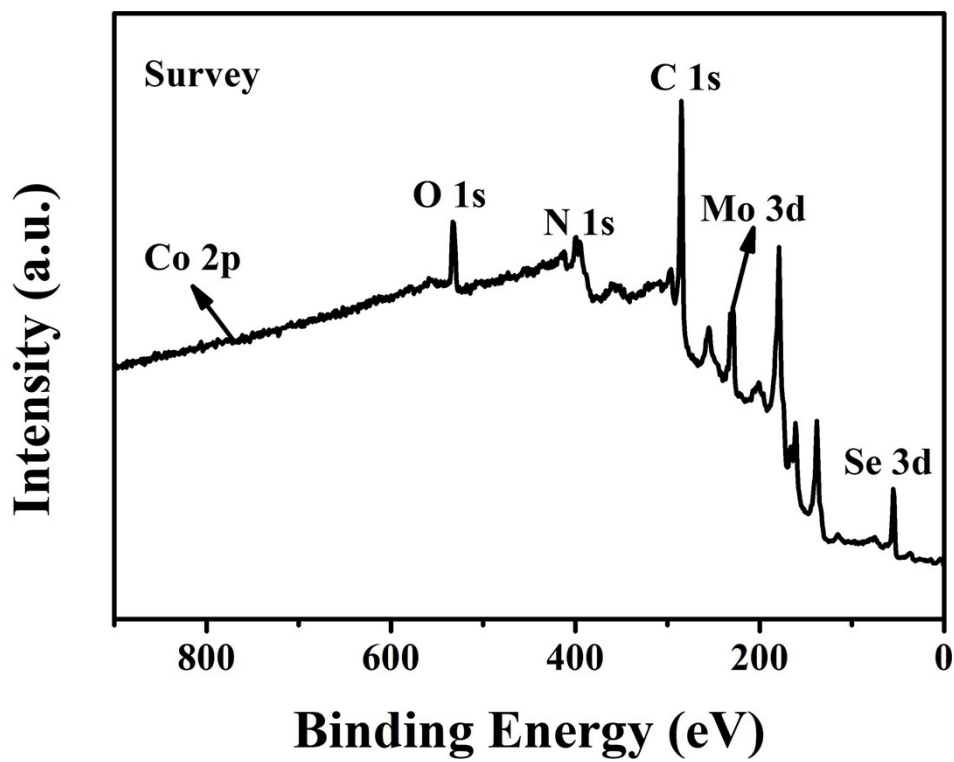


Figure S5. XPS spectra of Co-MoSe<sub>2</sub>@CN.

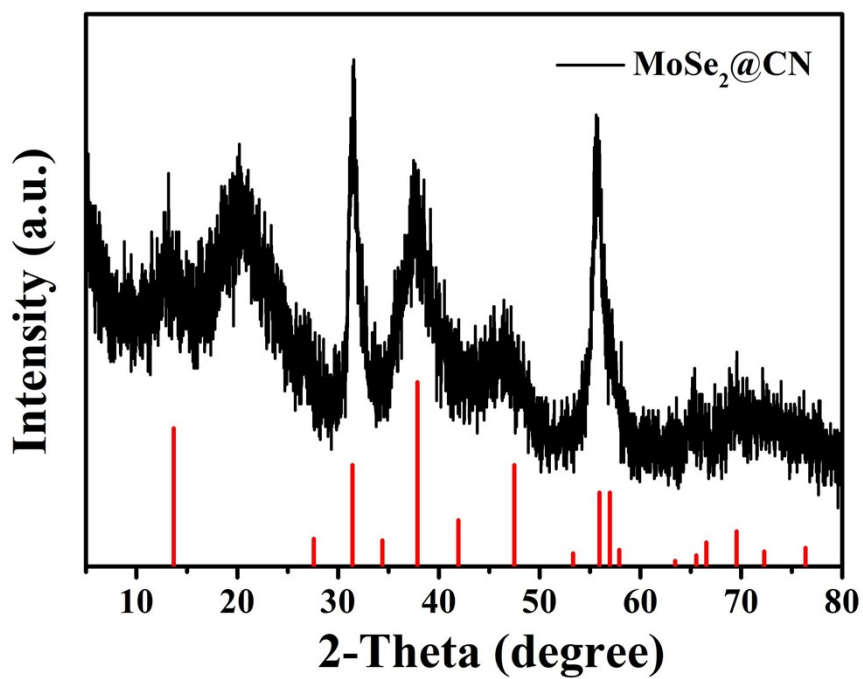
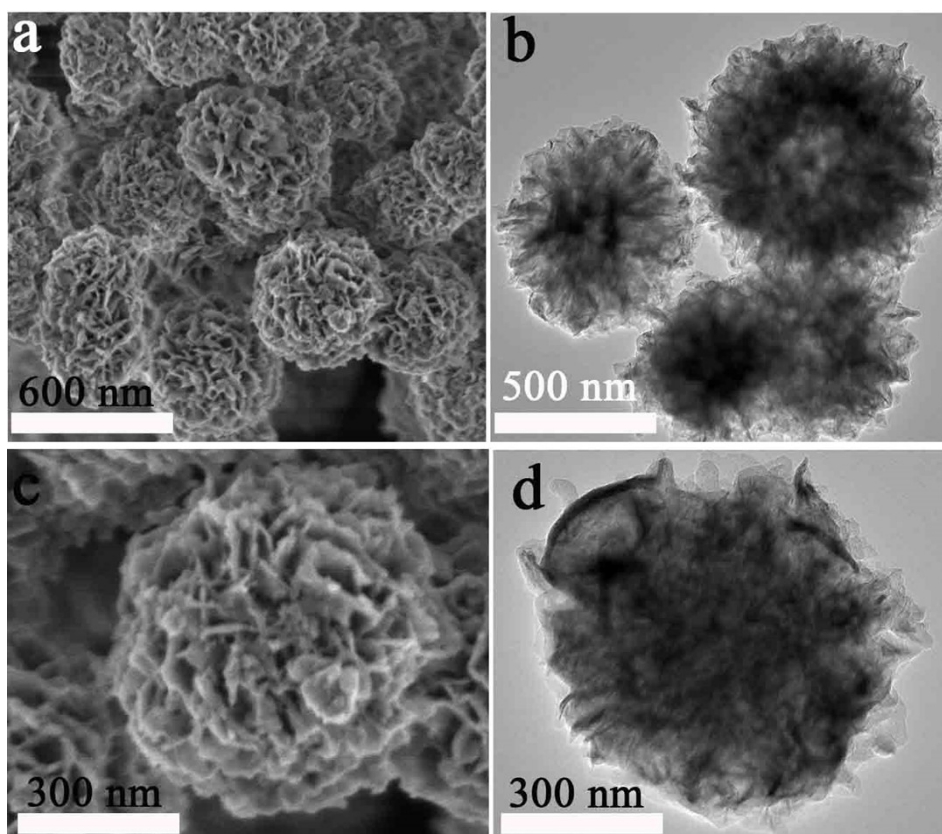
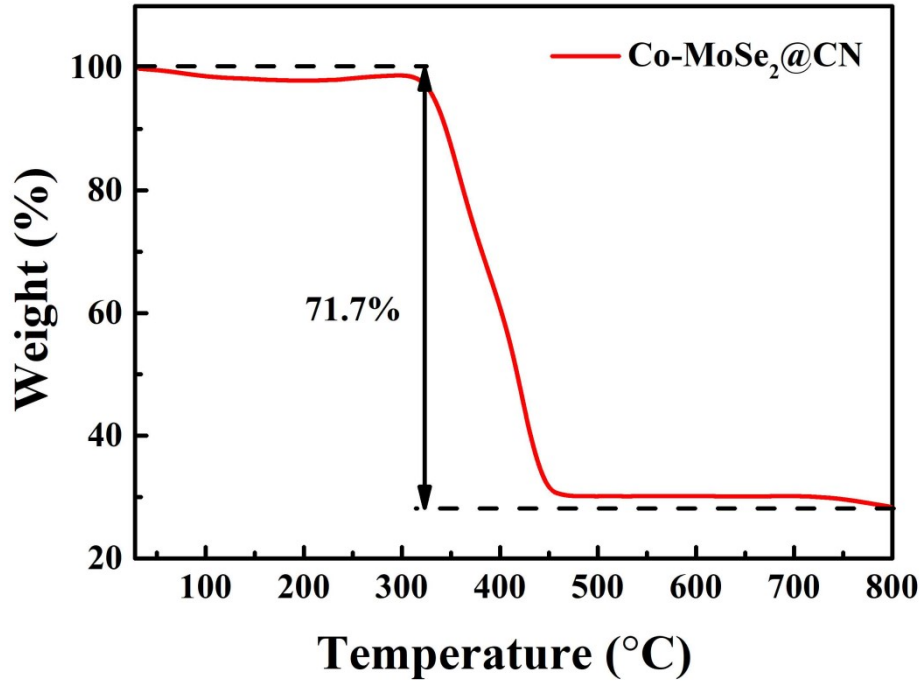


Figure S6. XRD pattern of MoSe<sub>2</sub>@CN.

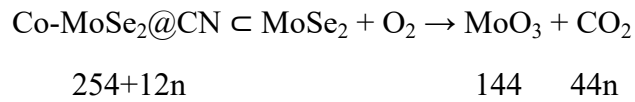


**Figure S7.** (a, c) SEM image of MoSe<sub>2</sub>@CN. (b, d) TEM image of MoSe<sub>2</sub>@CN.



**Figure S8.** TGA curve of Co-MoSe<sub>2</sub>@CN.

Through the TGA analysis, the carbon content can be obtained. And the calculating process is as following. We assume the mole ratio of C: Mo = n, and the Co content is ignored. During the TGA test in O<sub>2</sub> atmosphere, the corresponding oxidation reactions is as follows.



From this reaction, the weight loss ratio after calcination in O<sub>2</sub> atmosphere is as follows.

$$71.7\% = \frac{254 + 12n - 144}{254 + 12n}$$

$$n = 21.236$$

$$\frac{12 * 21.236}{254 + 12 * 21.236} = 50.08\%$$

So the carbon content in Co-MoSe<sub>2</sub>@CN is determined to be 50.08%.

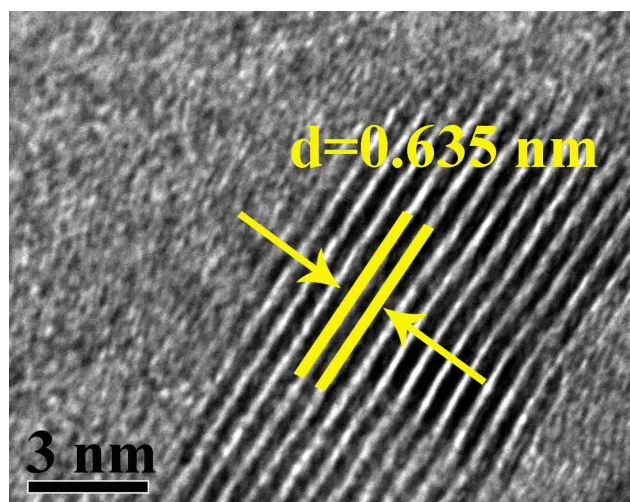


Figure S9. HRTEM image of MoSe<sub>2</sub>@CN.

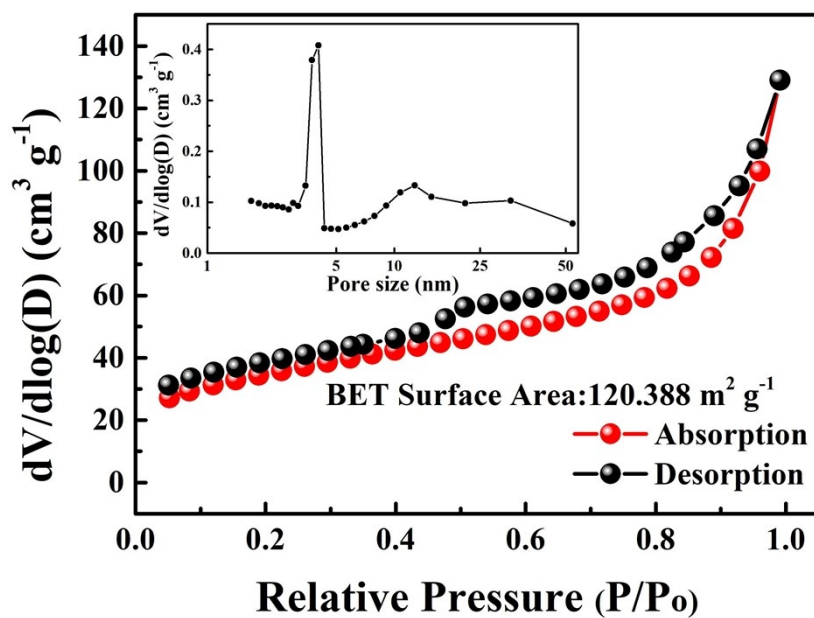


Figure S10. N<sub>2</sub> adsorption–desorption curves (the inset is BJH pore size distribution).

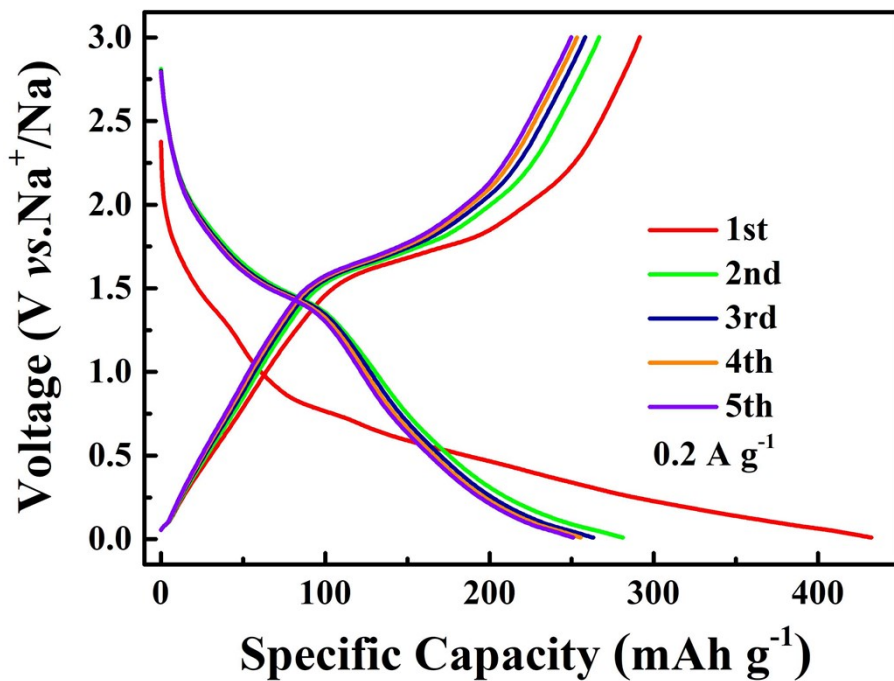


Figure S11. The discharge-charge curves at current densities of  $0.2 \text{ A g}^{-1}$  of  $\text{MoSe}_2@\text{CN}$ .

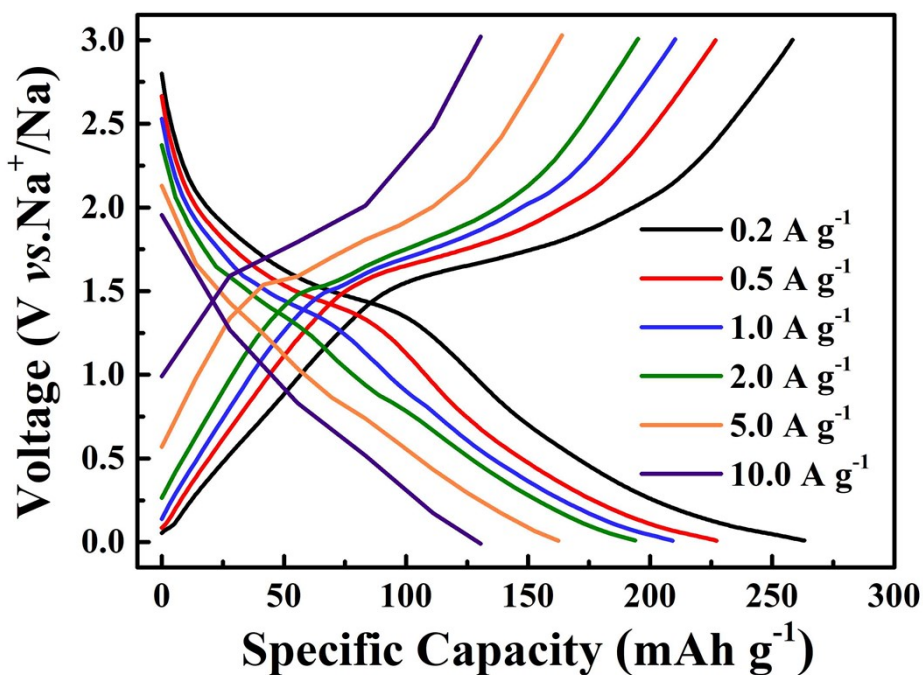


Figure S12. The discharge-charge curves at various current densities from  $0.2$  to  $10 \text{ A g}^{-1}$  of  $\text{MoSe}_2@\text{CN}$ .



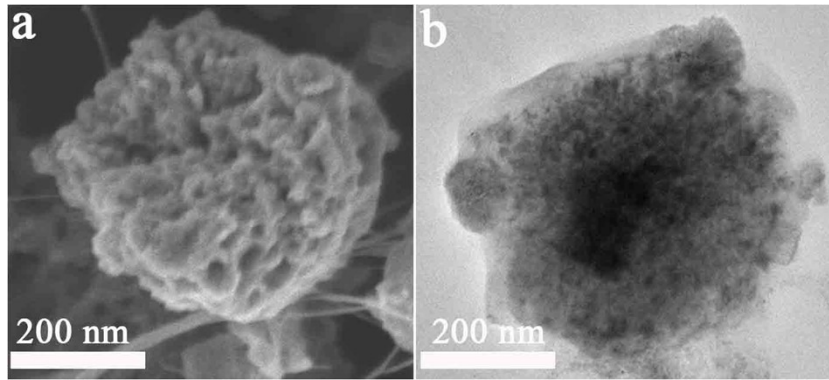


Figure S13. (a) SEM images and (b) TEM images of Co-MoSe<sub>2</sub>@CN after 50 cycles.

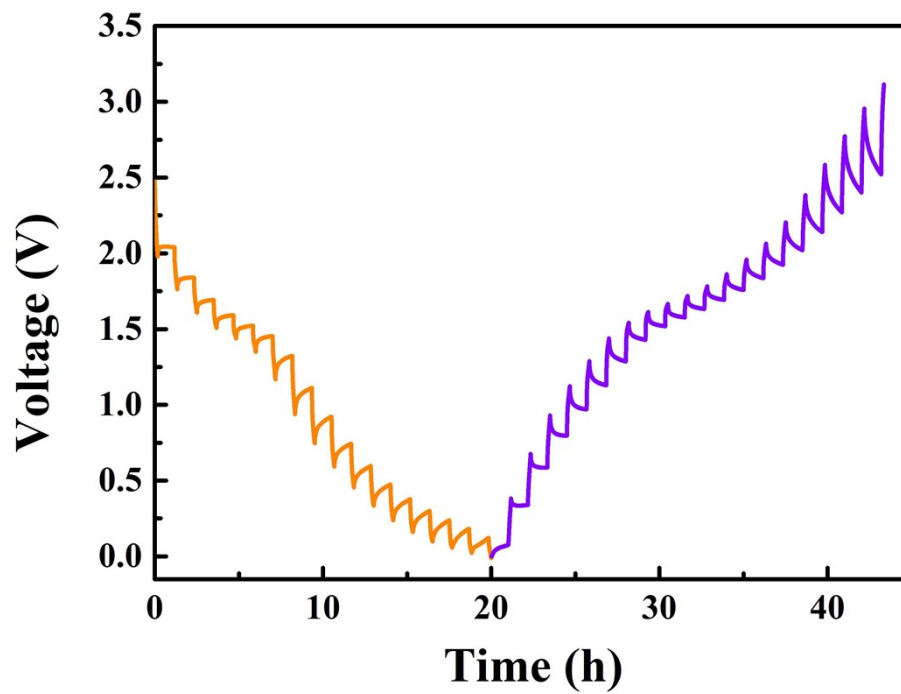
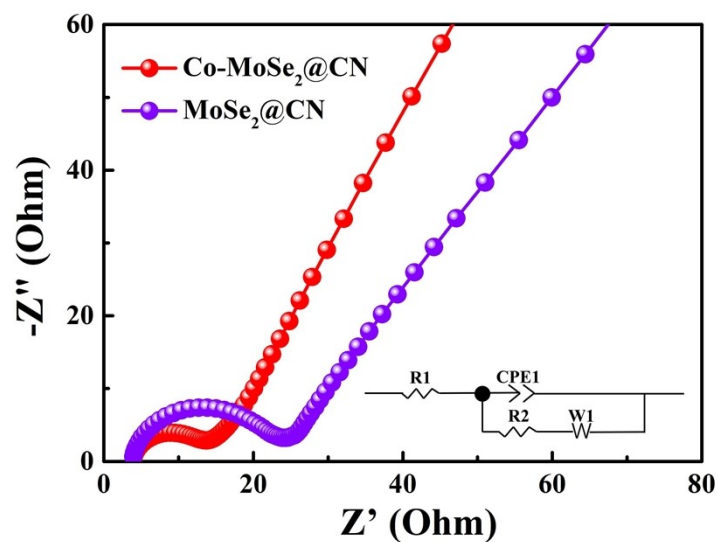
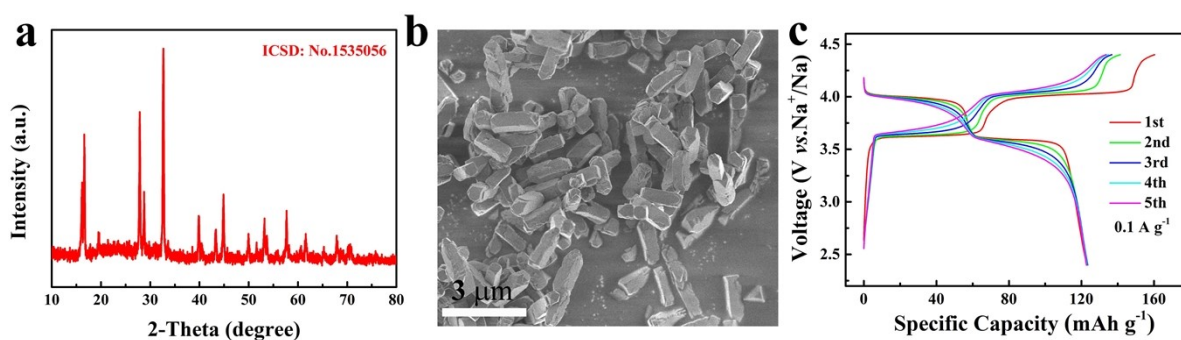


Figure S14. GITT curves of MoSe<sub>2</sub>@CN.



**Figure S15.** Nyquist plots of the Co-MoSe<sub>2</sub>@CN and MoSe<sub>2</sub>@CN.



**Figure S16.** The XRD pattern, SEM image and electrochemical performance of NVPOF (It was prepared as previously reported in *Inorg. Chem. Front.*, 2019, 6, 988-995).